



# Cancellation effect is present in high-frequency reversible and irreversible electroporation



Tamara Polajžer<sup>a</sup>, Janja Dermol-Černe<sup>a</sup>, Matej Reberšek<sup>a</sup>, Rodney O'Connor<sup>b</sup>, Damijan Miklavčič<sup>a,\*</sup>

<sup>a</sup> University of Ljubljana, Faculty of Electrical Engineering, Tržaška 25, 1000 Ljubljana, Slovenia

<sup>b</sup> École des Mines de Saint-Étienne, Department of Bioelectronics, Georges Charpak Campus, Centre Microélectronique de Provence, 880 Route de Mimet, 13120 Gardanne, France

## ARTICLE INFO

### Article history:

Received 15 July 2019

Received in revised form 3 December 2019

Accepted 5 December 2019

Available online 24 December 2019

### Keywords:

Electroporation  
Propidium iodide  
MTS assay  
PEF treatment  
Biphasic pulses

## ABSTRACT

It was recently suggested that applying high-frequency short biphasic pulses (HF-IRE) reduces pain and muscle contractions in electrochemotherapy and irreversible ablation treatments; however, higher amplitudes with HF-IRE pulses are required to achieve a similar effect as with monophasic pulses. HF-IRE pulses are in the range of a microsecond, thus, the so-called cancellation effect could be responsible for the need to apply pulses of higher amplitudes. In cancellation effect, the effect of first pulse is reduced by the second pulse of opposite polarity. We evaluated cancellation effect with high-frequency biphasic pulses on CHO-K1 in different electroporation buffers. We applied eight bursts of 1–10  $\mu$ s long pulses with inter-phase delays of 0.5  $\mu$ s – 10 ms and evaluated membrane permeability and cell survival. In permeability experiments, cancellation effect was not observed in low-conductivity buffer. Cancellation effect was, however, observed in treatments with high-frequency biphasic pulses looking at survival in all of the tested electroporation buffers. In general, cancellation effect depended on inter-phase delay as well as on pulse duration, *i.e.* longer pulses and longer interphase delay cause less pronounced cancellation effect. Cancellation effect could be partially explained by the assisted discharge and not by the hyperpolarization by the chloride channels.

© 2019 Elsevier B.V. All rights reserved.

## 1. Introduction

Electroporation is a phenomenon in which cells exposed to pulsed electric fields of a sufficient intensity form nanoscale defects referred to as pores in the cell membrane, where lipids are chemically modified and the function of membrane proteins is modulated [1]. Consequently, membrane permeability increases and allows molecules for which the membrane is usually impermeable to cross the cell membrane. If cells recover after treatment and survive, this is termed reversible electroporation. However, when damage is more extensive, and cells die, this is termed irreversible electroporation (IRE). Electroporation is used in medicine, *i.e.* electrochemotherapy (ECT) [2–5], gene therapy [6,7], DNA vaccination [8,9], and tumor [10,11] or cardiac ablation [12–15] by irreversible electroporation, in biotechnology [16–18], and food processing [16,19].

In ECT and IRE treatments, 50–100  $\mu$ s long monophasic pulses are traditionally applied at approximately 1 Hz repetition frequency, synchronized with the heart rhythm [4,11,20]. Low repetition frequency results in separate muscle contractions, *i.e.*

individual multiple muscle twitches associated with every pulse delivered [21]. Since pulses cause electrical stimulation of excitable tissue, also sensory nerves are stimulated, therefore the procedure is also painful for the patients [22,23]. Therefore, general anesthesia [24], synchronization with electrocardiogram [25–27] and administration of muscle relaxants are needed during the treatment to prevent painful muscle contraction.

It was previously suggested that unpleasant sensations could be reduced by increasing the pulse repetition frequency [23,28]. Although *in vitro* results were promising, as the obtained molecular uptake remained similar up to 8.3 kHz repetition frequency, only slightly higher voltages had to be applied with higher repetition frequencies [29]. *In vivo*, at 1 Hz a higher percentage of complete tumor regression was observed than at 5 kHz repetition frequency, especially when using sub-optimal drug concentrations [28,30]. Another suggestion to reduce muscle and nerve excitation and elevate pain was to use specially designed electrodes, *i.e.* insulated needle electrodes [31] or “current cage” electrode placement [32]. Another recent approach was to replace the standard 50–100  $\mu$ s monophasic pulses by bursts of short biphasic pulses, the so-called high-frequency irreversible electroporation (HF-IRE). When HF-IRE pulses were applied *ex-vivo* and *in vivo* to several animal models [33–35] as well as to humans in the first human

\* Corresponding author.

E-mail address: [Damijan.miklavcic@fe.uni-lj.si](mailto:Damijan.miklavcic@fe.uni-lj.si) (D. Miklavčič).

study on prostate cancer [36], there were fewer muscle contractions observed and less muscle relaxants needed than in standard IRE treatments. The efficiency of the HF-IRE treatment was comparable to the IRE treatment; however, higher amplitudes of electric pulses had to be in the HF-IRE treatments than when using standard IRE pulses. Nevertheless HF-IRE pulse treatments could potentially improve the procedural safety for patients by obviating the need for neuromuscular blockage and general anesthesia.

In addition to IRE it was also demonstrated that high-frequency electroporation, *i.e.* HF-EP with bursts of short biphasic pulses could be used to increase membrane permeability to fluorescent dyes [37] and recently, also to chemotherapeutic cisplatin in electrochemotherapy *in vitro* [38]. However, in this case higher electric pulses had to be delivered with HF-EP than with classical  $8 \times 100 \mu\text{s}$  ECT to achieve a comparable effect for equal pulse duration.

It was previously reported that biphasic pulses were at least as efficient as monophasic pulses. *In vitro*, higher DNA transfection efficiency was obtained with biphasic pulses than with monophasic pulses [39]. Presumably, biphasic pulses induced cell membrane permeabilization on both sides of the membrane facing the electrodes and not only on one side, as would be expected with monophasic pulses. Improved efficiency of permeabilization with biphasic pulses was later confirmed also by increased membrane permeability [40], while the electrolytic contamination with biphasic pulses was lower than with monophasic pulses [41]. *In vivo*, monophasic (100  $\mu\text{s}$ ) and biphasic pulses (50 + 50  $\mu\text{s}$ ) were reported to be of similar efficiency in electrochemotherapy [42], whilst with 20 ms long biphasic pulses a higher transgene expression in liver tissue was obtained than with unipolar pulses (monophasic) [43]. In another study, no difference was seen in gene transfer of skin between applying monophasic and biphasic pulses [44]. In all studies mentioned above, however, longer pulses were applied than those used in HF-IRE (>10  $\mu\text{s}$ ).

Over time, the development of new pulse generators has made it possible to deliver even shorter pulses in the nanosecond time range [45]. Interesting new observations were made using biphasic nanosecond pulses suggesting they were less efficient in permeabilizing and killing cells than monophasic nanosecond pulses [46], *i.e.* the so-called cancellation effect was observed which challenged the existing knowledge. Briefly, a cancellation effect was reported in which the effect of the first pulse was cancelled (or reduced) by the effect of the second pulse of the opposite polarity, although applying asymmetrical biphasic pulses (in voltage [47] and time [48]) decreases the extent of the cancellation effect. This cancellation effect was observed for one or more biphasic pulses with the duration of the positive or the negative pulse between 60 and 900 ns and the delay between the positive and the negative pulse up to 10 ms [46–51]. It was detected via calcium influx, the influx of fluorescent dyes, phosphatidylserine externalization, metabolic assays of survival, and membrane conductance measurements. The reason(s) for this cancellation effect have not yet been identified; however, different theories and models were proposed [52,53]. The mechanisms suggested are: assisted membrane discharge; reversed electrophoretic ion transport; two-step oxidation of membrane phospholipids [49]; localized charging and discharging events across the membrane [48]; and reversed elongation forces due to electrodeformation [51,54]; but evidence supporting each of these mechanisms are lacking. Here, we investigated a new hypothesis – a hyperpolarization of chloride channels.

Chloride channels (CLC) are responsible for the movement of  $\text{Cl}^-$  ions necessary in neuronal, muscular, cardiovascular, and epithelial function [55]. CLC channels are dimers with each of the subunits forming ‘protopores’ that combined together leads to two types of gating, slow and fast [56]. Unlike most other types of voltage-gated ion channels, their structure does not include an

S1-S4 transmembrane voltage-sensing motif. Instead, their fast gating voltage dependence arises from the movement of the permeant  $\text{Cl}^-$  ion through the transmembrane electric field, which interestingly can be activated by either hyperpolarization or depolarization. Consequently, CLC channels can exhibit bidirectional ultrafast gating of  $\text{Cl}^-$  in the  $\mu\text{s}$  range that is dependent on the concentration of extracellular  $\text{Cl}^-$ . We hypothesized that the transit of  $\text{Cl}^-$  in the pores of CLC channels might therefore be sensitive to the rapid reversal of electric field in biphasic pulses, leading to the cancellation effect.

Since pulses, usually applied in HF-IRE treatments are biphasic and 1  $\mu\text{s}$  long, they are already in the time range of the cancellation effect. Thus, in our study, we aimed to determine if the cancellation effect is also present in HF-IRE treatments *in vitro*. The cancellation effect could partially explain why higher voltages must be applied with HF-IRE pulses than with IRE pulses to achieve a comparable effect. We evaluated irreversible as well as reversible electroporation, and thus we call our protocol high-frequency electroporation (HF-EP). We varied pulse duration between 1 and 10  $\mu\text{s}$ , while the inter-phase delay was varied between 0.5  $\mu\text{s}$  – 10 ms. We compared the effect of HF-EP pulses to standard IRE or ECT pulses (*i.e.* 100  $\mu\text{s}$  monophasic pulses) with the same total pulse duration. Experiments were performed in three different electroporation buffers, as it was already shown that electroporation buffers significantly influence electroporation experiments [57]. We also performed calculations where we evaluated the effect of buffer conductivity on membrane charging and discharging. Our results show that the cancellation effect is present in HF-EP treatments and shows its complex dependency on the electroporation buffer.

## 2. Materials and methods

### 2.1. Electroporation buffers

Three different electroporation buffers were used (Table 1). A standard low-conductivity potassium-phosphate (KPB) buffer is often used in *in vitro* experiments due to current limitations of pulse generators. To obtain the high-conductivity buffer, we iso-osmotically replaced the sucrose by NaCl as sucrose is physiologically not present at high concentrations. To obtain the buffer without chloride, MgCl was replaced by magnesium D-gluconate hydrate and NaCl by sodium gluconate. We eliminated all chloride ions to test a hypothesis that the cancellation effect could be explained by hyperpolarization of the cell membrane caused by the activation of chloride channels. All buffers were iso-osmotic (300 mOsm/kg), as determined by freezing point depression method with Knauer cryoscopic unit (model 7312400000, Knauer,

**Table 1**  
Composition and electrical conductivity of three electroporation buffers, used in our study.

Electroporation buffer	Composition	Electrical conductivity (mS/cm)
Low-conductivity buffer	10 mM $\text{K}_2\text{HPO}_4/\text{KH}_2\text{PO}_4$ in ratio 40.5:9.5, 1 mM $\text{MgCl}_2$ , 250 mM $\text{C}_{12}\text{H}_{22}\text{O}_{11}$	1.76 [57]
High-conductivity buffer	10 mM $\text{K}_2\text{HPO}_4/\text{KH}_2\text{PO}_4$ in ratio 40.5:9.5 1 mM $\text{MgCl}_2$ , 150 mM NaCl	19.12 [57]
Buffer without chloride	10 mM $\text{K}_2\text{HPO}_4/\text{KH}_2\text{PO}_4$ in ratio 40.5:9.5, 1 mM $\text{C}_{12}\text{H}_{22}\text{MgO}_{14} \cdot x\text{H}_2\text{O}$ , 150 mM $\text{NaC}_6\text{H}_{11}\text{O}_7$	9.57*

\* Measured with the conductometer S230 SevenCompact (Mettler Toledo, Switzerland) at room temperature (24 °C).

Germany). All chemicals were from Sigma Aldrich, Germany, except for  $\text{KH}_2\text{PO}_4$ , which was from Merck, Germany.

## 2.2. Cell preparation

Chinese hamster ovary (CHO-K1) cells purchased from the European Collection of Authenticated Cell Cultures were grown in HAM F-12 growth medium (PAA, Austria) in culture flasks (TPP, Switzerland) in an incubator (Kambič, Slovenia) at 37 °C with a humidified 5%  $\text{CO}_2$ . The growth medium was supplemented with 10% fetal bovine serum (Sigma-Aldrich, Germany), L-glutamine (StemCell, Canada), antibiotics penicillin/streptomycin (PAA, Austria) and gentamycin (Sigma-Aldrich, Germany) (i.e., full HAM-F12). After 2–3 days when 70% confluency was reached, cells were detached by 10x trypsin-EDTA (PAA, Austria), diluted 1:9 in Hank's basal salt solution (StemCell, Canada), which was inactivated after 2 min by addition of fresh full HAM F-12. The cell suspension was centrifuged at 180 g and 22 °C for 5 min. The supernatant was removed, and the cell pellet was re-suspended in the chosen electroporation buffer at the cell density  $2 \times 10^6$  cells/ml.

## 2.3. Pulse generation

Pulses were applied by a laboratory prototype pulse generator (University of Ljubljana), based on H-bridge digital amplifier with 1 kV MOSFETs (DE275-102N06A, IXYS, USA) [37]. Two types of pulses were delivered – monophasic pulses and bursts of biphasic pulses (HF-EP treatment). We adopted the nomenclature from the field of cardiac ablation where bipolar pulses are called biphasic pulses and the delay between the pulses is the inter-phase delay. Pulses were delivered between stainless steel 304 plate electrodes with 2 mm interelectrode distance. Between samples, electrodes were cleaned in experimental electroporation buffer and dried with sterile gauze. Control sample was subjected to the same procedure of the exposed sample in absence of pulses, i.e. 0 V/cm amplitude. Monophasic square pulse treatment consisted of eight 100  $\mu\text{s}$  long pulses of 100–1000 V (resulting in voltage-to-distance ratio: 0.5–5 kV/cm) delivered in a step of 100 V at 1 Hz pulse repetition frequency and was used as a reference for standard electroporation protocols. In HF-EP treatment (Schematic 1, Table 2), eight bursts were applied at 1 Hz repetition frequency. Each burst consisted of several biphasic pulses. One biphasic pulse consisted of a negative and a positive pulse, both of lengths 1, 5 or

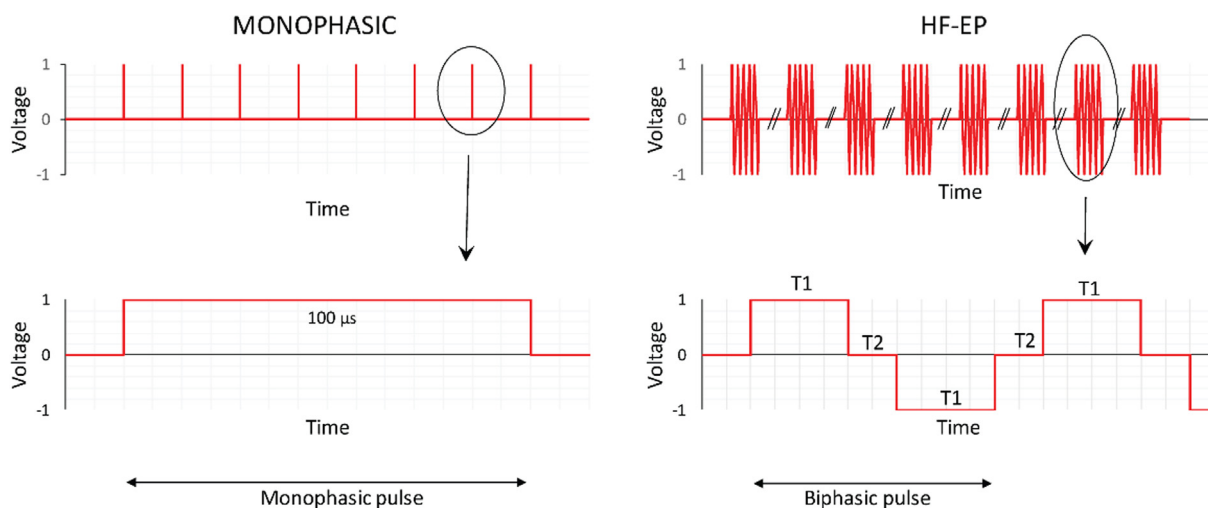
10  $\mu\text{s}$  (T1) and voltage 100 – 1000 V, delivered in a step of 100 V. The inter-phase delay and the delay between biphasic pulses was 0.5  $\mu\text{s}$  – 10 ms (T2) (see Table 2), i.e. delay lengths already studied in cancellation effect [49,50]. The number of biphasic pulses and their duration in one burst was adapted to obtain a total on-time of 100  $\mu\text{s}$  (see Table 2). The total on-time of HF-EP pulse treatment was thus equivalent to the monophasic pulse treatment ( $\Sigma = 800 \mu\text{s}$ ). The delivered voltage and current was measured with an oscilloscope, Wavesurfer 422, 200 MHz, using a differential probe (ADP305) and current probe (CP030) (all from LeCroy, USA) (see Fig. 1). The current in low-conductivity buffer was measured up to 1000 V, however, in high-conductivity buffer and in buffer without chloride the highest measured voltage was 700 V, as higher voltages resulted in currents above 30 A which could damage the current probe.

## 2.4. Permeabilization assay

Just before electric pulses were applied, 50  $\mu\text{l}$  of cells suspension was mixed with propidium iodide (PI, Life Technologies) to obtain a final concentration of 100  $\mu\text{g/ml}$ . The sample was transferred between electrodes, and electric pulses were applied. The sample was transferred to a 1.5 ml tube and incubated at room temperature for three minutes. Afterwards, 150  $\mu\text{l}$  of electroporation buffer was added to obtain a high-enough volume for measurement. The uptake of PI was detected by flow cytometry (Attune NxT; Life Technologies, Carlsbad, CA, USA). Samples were excited with a blue laser at 488 nm and emitted fluorescence was detected through a 574/26 nm band-pass filter. 10,000 events were obtained, and data were analyzed using the Attune Nxt software. On the dot-plots of forward-scatter and side-scatter, single cells were separated from debris and clusters. The percentage of PI permeabilized cells was obtained from the PI fluorescence intensity histogram, by gating permeabilized from non-permeabilized cells. Each data point was repeated three times.

## 2.5. Viability assay

50  $\mu\text{l}$  samples of cell suspension were transferred between the electrodes, and electric pulses were applied. Afterwards, 40  $\mu\text{l}$  of the electroporated cell suspension was diluted in full HAM-F12 growth media to obtain cell density  $2 \times 10^4$  cells/100  $\mu\text{l}$ . 100  $\mu\text{l}$



**Schematic 1.** Scheme of the pulses applied in experiments. On the left is the pulse shape of standard monophasic pulse treatment (8 monophasic pulses of 100  $\mu\text{s}$ ) and on the right is the pulse shape of HF-EP pulse treatment. One burst consists of several biphasic pulses. We varied pulse length (T1), inter-phase delays (T2), while the on-time of each burst was fixed to 100  $\mu\text{s}$  by number of pulses in one burst.

**Table 2**  
Description of the HF-EP pulse parameters. Total on-time in one burst was the same as in one 100  $\mu\text{s}$  monophasic pulse since  $\text{pulse length} \times 2$  (positive and negative part of a biphasic pulse)  $\times$  number of biphasic pulses = 100  $\mu\text{s}$ .

Pulse length ( $\mu\text{s}$ ) – T1	Inter-phase delay ( $\mu\text{s}$ ) – T2	Number of biphasic pulses in one burst (–)	Applied voltage (V)	Total time ( $\mu\text{s}$ )
1	0.5, 1, 5, 10, 100, 1000, 10,000	50	100–1000 V in a step of 100 V	100
5	0.5, 1, 5, 10, 100, 1000, 10,000	10	100–1000 V in a step of 100 V	100
10	0.5, 1, 5, 10, 100, 1000, 10,000	5	100–1000 V in a step of 100 V	100

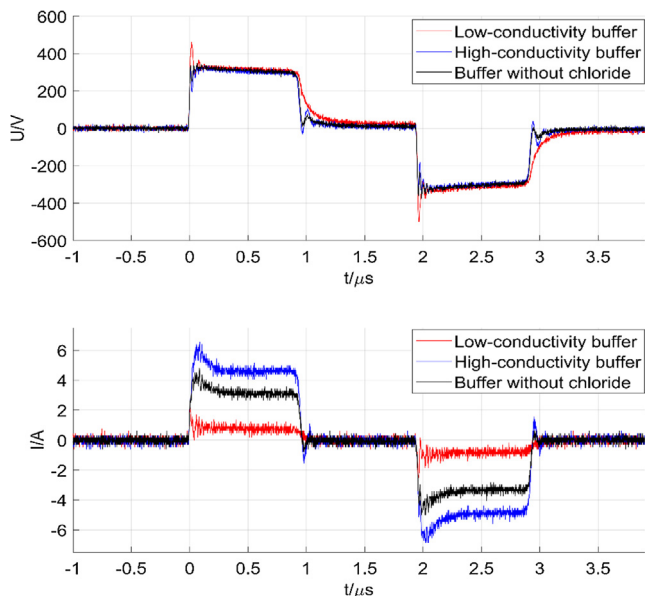


**Fig. 1.** Measured voltage and current of pulses in different buffers. The waveform of one biphasic pulse with the duration T1 of 1  $\mu\text{s}$  and inter-phase delay T2 of 1  $\mu\text{s}$  320 V (1.6 kV/cm) were applied. Waveforms in different buffers are shown in correspondent colors (low-conductivity buffer in red, high-conductivity in blue and buffer without chloride in black). (For interpretation of the references to color in this figure legend, the reader is referred to the web version of this article.)

of cell suspension was then transferred (in three technical repetitions) to wells in the 96-well plate and incubated at 37  $^{\circ}\text{C}$  and humidified 5%  $\text{CO}_2$  atmosphere. MTS assay (CellTiter 96<sup>®</sup> Aqueous One Solution Cell Proliferation Assay, Promega, USA) was used to assess cell viability 24 h after electric pulses were applied. 20  $\mu\text{l}$  of MTS tetrazolium reagent was added to the samples, and the 96-well plate was returned to the incubator for 2.5 h. The absorbance of formazan (reduced MTS tetrazolium compound) was measured with a spectrofluorometer (Tecan Infinite M200, Tecan, Austria) at 490 nm. Each data point was repeated three times. Background absorbance was subtracted for all the samples and control and the percentage of viable cells was calculated by subtracting the background and normalizing the absorbance of the samples to the absorbance of the control (0 V/cm).

## 2.6. Temperature measurement

50  $\mu\text{l}$  of all three electroporation buffers was transferred between the stainless steel plate electrodes ( $d = 2$  mm). Experiments were performed at room temperature (24  $^{\circ}\text{C}$ ). Temperature changes were measured by the fiber optic sensor system (opSens, Québec, Canada), with a temperature probe (ProSens, opSens), which consisted of ProSens signal conditioner and a fiber optic temperature sensor OTG-M170 with a diameter of 0.17 mm. The sensor was placed in the drop between the electrodes. The temperature was measured before, during and 10 s after electric pulse delivery. With biphasic pulses, we tested bursts of 1, 5 and 10  $\mu\text{s}$

long pulses and applied 320 V (voltage in permeability experiments), 600 V (voltage in survival experiments) and 1000 V (maximal applied voltage) with the same pulse and burst number as in permeability and survival experiments. We chose 0.5  $\mu\text{s}$  as the inter-phase delay to have the smallest heat dissipation between pulses, i.e. the worst-case scenario. We also applied eight 100  $\mu\text{s}$  long monophasic pulses at 320 V, 600 V and 1000 V.

## 2.7. Statistical analysis

Statistical analysis was performed using Graphpad Prism 7 (Graphpad software, San Diego, USA). The results are expressed as mean  $\pm$  SD, and statistically significant differences (\* $p < 0.05$ , \*\* $p < 0.01$ , \*\*\* $p < 0.001$ ) were determined by one-way ANOVA with Tukey's multiple comparisons test.

## 2.8. Calculation

We conducted a theoretical analysis of the time course of transmembrane voltage induced by square pulses, as described in [58]. For the induced transmembrane voltage ( $\Delta\Phi_m$ ) in response to a step turn-on of the DC field, we presumed the exponential shape of increase in the ITV on a single spherical cell:

$$\Delta\Phi_m(t) = fER \cos\theta \left( 1 - \exp\left(-\frac{t}{\tau}\right) \right) \quad (1)$$

With the time constant  $\tau$  being defined as

$$\tau = \frac{RC_m}{\frac{2\lambda_0\lambda_1}{2\lambda_0+\lambda_1} + \frac{R}{d}\lambda_m} \quad (2)$$

where  $\lambda_0$ ,  $\lambda_i$ , and  $\lambda_m$  are extracellular, intracellular and membrane conductivity, respectively,  $R$  cell radius (flow cytometry analysis showed no difference in FSC scatter of cells in low-conductivity buffer, high-conductivity buffer or buffer without chloride, i.e. buffers did not cause cells to shrink or swell),  $d$  cell membrane thickness,  $C_m$  membrane capacitance,  $E$  applied electric field,  $f$  the geometrical factor (approx. 1.5),  $\theta$  the angle between the electric field from the center of the sphere to a point on the cell membrane.

Square pulses consist of two steps (turn-on and turn-off), and thus the response is a superposition of the two separate responses. If several pulses are applied, the response is a superposition of responses to each pulse separately (Fig. 7 in [58]). For the calculations, we used equations (9a-f), (A6d) and (A8) from [58], and the reader is advised to search there for the details of our calculation. Calculations were performed in Matlab R2017 (Mathworks, USA).

In our experiments, cells were electroporated in three different buffers. From Eq. (2) we can see that the time constant also depends on the electric conductivity of the extracellular liquid ( $\lambda_0$ ). The parameters used in our calculations and their values are given in Table 3. The values (except for the extracellular conductivity, which was determined experimentally in the scope of our study) were all taken from [58]. The results are reported as ITV normalized to  $fER$ .

**Table 3**

Parameters used in our calculations, their symbols and values.

Parameter	Symbol	Value
Cell radius	$R$	10 $\mu\text{m}$
Membrane capacitance	$C_m$	$\epsilon_m/d = 8.8 \text{ F/m}^2$
Cytoplasmic conductivity	$A_i$	0.3 S/m
Cytoplasmic permittivity	$\epsilon_i$	$7.1 \times 10^{-10} \text{ As/Vm}$
Membrane conductivity	$A_m$	$3 \times 10^{-7} \text{ S/m}$
Membrane permittivity	$\epsilon_m$	$4.4 \times 10^{-11} \text{ As/Vm}$
Membrane thickness	$d$	5 nm
Conductivity of the electroporation buffer	$\lambda_o$	$\lambda_1 = 1.76 \text{ mS/cm}$ $\lambda_2 = 19.12 \text{ mS/cm}$ $\lambda_3 = 9.57 \text{ mS/cm}$

### 3. Results

#### 3.1. Cancellation effect as a function of the amplitude of the electric field

First, we focused on cell survival (Fig. 2) as HF-IRE pulses are predominantly used to achieve irreversible electroporation. Then, we determined cell membrane permeability (Fig. 3), as we aim to use HF-EP also to achieve reversible electroporation. Both cell survival and cell membrane permeabilization were evaluated as a function of electric field amplitude for monophasic pulses and for HF-EP pulses when pulse length (T1) was 1  $\mu\text{s}$ , and the inter-phase delay (T2) was 1  $\mu\text{s}$  or 10 ms. Three different electroporation buffers were used to observe buffer dependency.

Monophasic pulses were more efficient than biphasic pulses in survival and permeability experiments, as they caused higher cell membrane permeabilization and lower survival at the same electric fields (Figs. 2 and 3).

In Fig. 2 we can see that the cancellation effect was consistently observed in all three buffers when cell survival was evaluated. Namely, when the inter-phase delay was 10 ms (dashed lines),

pulses were more effective at decreasing cell survival, and lower electric fields were needed to achieve the same cell death than with 1  $\mu\text{s}$  (solid lines) inter-phase delay.

On the contrary in permeability experiments, we observed either a cancellation or a sensitization effect (Fig. 3). A cancellation effect was present in the high-conductivity buffer and the buffer without chloride, as HF-EP pulse treatment with a longer inter-phase delay (10 ms) was more efficient than HF-EP pulse treatment with a shorter inter-phase delay (1  $\mu\text{s}$ ) between pulses at the same electric field. However, in the low-conductivity buffer, we observed that HF-EP pulse treatment with a shorter inter-phase delay (1  $\mu\text{s}$ ) between pulses was more efficient than HF-EP pulse treatment with a longer inter-phase delay (10 ms) between pulses at the same electric field, *i.e.* we observed the 'sensitization' effect, similar as in [57].

#### 3.2. Cancellation effect as a function of pulse duration and inter-phase delay

The cancellation effect in HF-EP treatment was studied in detail by applying 1, 5 and 10  $\mu\text{s}$  long pulses (T1) with several different inter-phase delays (0.5  $\mu\text{s}$  – 10 ms) (T2) (Fig. 4), again by evaluating cell survival and cell membrane permeabilization. We applied a fixed voltage of 600 V, *i.e.* 3000 V/cm between the electrodes in survival experiments and 320 V *i.e.* 1600 V/cm in permeability experiments. As our hypothesis about the contribution of voltage-gated chloride ions was disproved, these experiments were performed only in the low- and high-conductivity buffer.

Longer pulses (10  $\mu\text{s}$ ) were more efficient than shorter pulses (1  $\mu\text{s}$ ) in achieving cell membrane permeabilization and cell death, irrespective of the inter-phase delay T2 and the buffer.

In the low-conductivity buffer, no cancellation effect was present in permeabilization or survival. On the contrary, for pulse duration T1 = 1  $\mu\text{s}$ , cell permeabilization was less efficient when the inter-phase delay was increased, *i.e.*, we observed a sensitiza-

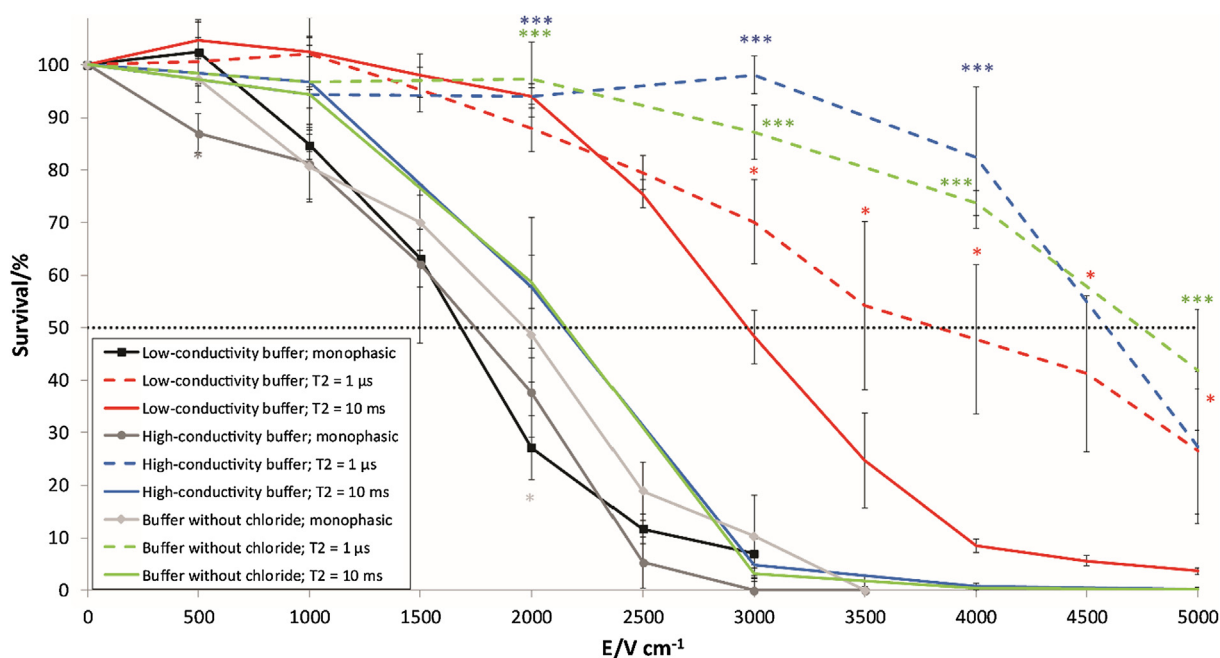


**Fig. 2.** Cell survival as a function of the electric field in three different buffers. In HF-IRE treatment, pulse duration was 1  $\mu\text{s}$ , and the inter-phase delay was either 1  $\mu\text{s}$  or 10 ms. Monophasic pulses are shown in solid black, dark grey and light grey lines for low-conductivity buffer, high-conductivity buffer and buffer without chloride. HF-IRE pulses with T1 = 1  $\mu\text{s}$  are shown in red, blue and green for low-conductivity buffer, high-conductivity buffer and buffer without chloride, respectively. Dashed lines (---) are used for pulses with 1  $\mu\text{s}$  inter-phase delay and solid lines (—) for 10 ms. 50% survival is shown in a dotted line (.....). Results are shown as mean  $\pm$  standard deviation. The asterisks (\*) mark  $p < 0.05$ ,  $p < 0.01$ \*\*,  $p < 0.001$ \*\*\* and show statistically significant differences between monophasic pulses and different T2 of the same buffer in HF-IRE pulses. (For interpretation of the references to color in this figure legend, the reader is referred to the web version of this article.)

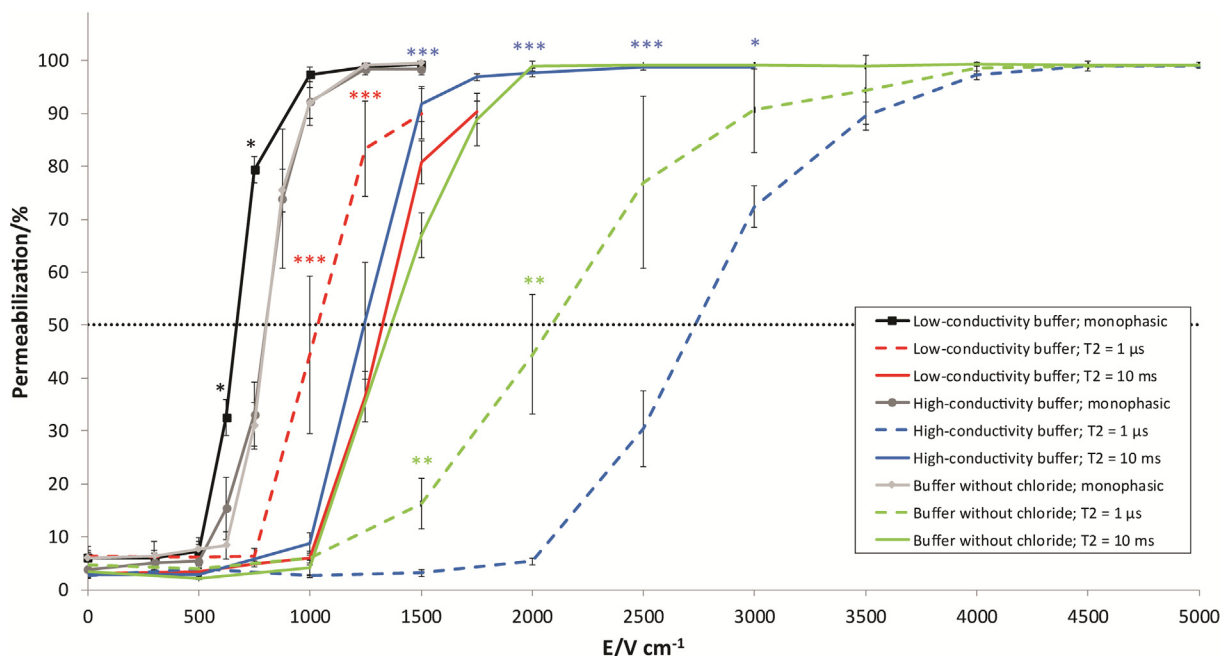


**Fig. 3.** Cell membrane permeabilization as a function of the applied electric field in different buffers. In HF-EP treatment, pulse duration was 1  $\mu\text{s}$ , and the inter-phase delay was either 1  $\mu\text{s}$  or 10 ms. Monophasic pulses are shown in solid black, dark grey and light grey lines for low-conductivity buffer, high-conductivity buffer and buffer without chloride. HF-EP pulses with  $T_1 = 1 \mu\text{s}$  are shown in red, blue and green, for low-conductivity buffer, high-conductivity buffer and buffer without chloride, respectively. Dashed lines (---) are used for pulses with 1  $\mu\text{s}$  inter-phase delay and solid lines (—) for 10 ms. 50% permeabilization is shown in a dotted line (.....). Results are shown as mean  $\pm$  standard deviation. The asterisks (\*) mark  $p < 0.05^*$ ,  $p < 0.01^{**}$ ,  $p < 0.001^{***}$  and show statistically significant differences between monophasic pulses and between different  $T_2$  of the same buffer. (For interpretation of the references to color in this figure legend, the reader is referred to the web version of this article.)

tion effect (Fig. 4b). For cell membrane permeabilization with 5 and 10  $\mu\text{s}$  long pulses, the sensitization effect was observed only with longer inter-phase delays of 1 ms and 10 ms. In high-conductivity buffer, however, longer inter-phase delays ( $T_2$ ) were more efficient in permeabilizing and killing cells than shorter, *i.e.* a cancellation effect was present and decreased with longer  $T_2$  (statistical difference between  $T_2 = 0.5 \mu\text{s}$  and  $T_2 = 1000 \mu\text{s}$  or more is  $p < 0.001$ ) (Fig. 4d). The extent of the cancellation was reduced with an increase in pulse duration ( $T_1$ ). Interestingly, the cancellation effect in survival assay was still observed at 10  $\mu\text{s}$ , the longest pulse length tested (Fig. 4c).

### 3.3. Temperature measurements

Fig. S1 shows the time dependency of temperature when HF-EP or ECT pulses are applied. We can see that in high-conductivity buffer and in buffer without chloride during each burst, the temperature increases and during the delay between bursts, it decreases.

In Table S1, the maximal temperature is shown for various combinations of pulse parameters and electroporation buffers. We can see that the maximal increase was 23  $^{\circ}\text{C}$  when 1000 V was applied.

### 3.4. Calculation of the assisted discharge

Assisted discharge was suggested as one of the possible mechanisms responsible for the cancellation effect [49]. The time-constant of the membrane depends, amongst other factors, on the extracellular conductivity, which varied between our buffers (Table 1). Fig. S2 shows the membrane time constant (calculated according to Eq. (1)) as a function of extracellular conductivity with marked time constants for the three buffers, used in our study.

In Fig. 5, we can see that with longer inter-phase delays (5  $\mu\text{s}$  or more) the membrane discharges completely and there is no contribution of the assisted discharge. In Fig. 6, we can see that with 5  $\mu\text{s}$  pulses, we reach stationary transmembrane voltage during the pulse application, *i.e.* the membrane charges completely. Similarly as in Fig. 5 with 1  $\mu\text{s}$  pulses, we can see that with the inter-phase delays of 0.5 and 1  $\mu\text{s}$  the membrane does not discharge completely, but with inter-phase delays of 5  $\mu\text{s}$  it does. From Figs. 5, 6 and Table 4 we can observe that cell membranes charge and discharge slowest in the low-conductivity buffer and in all three buffers, it takes maximally 5  $\mu\text{s}$  to charge/discharge.

## 4. Discussion

In our study, we evaluated the cancellation effect in *in vitro* experiments with high-frequency short biphasic pulses, *i.e.*, high-frequency electroporation (HF-EP), by determining cell survival and cell membrane permeability in three different electroporation buffers across a wide range of pulse parameters. In HF-EP, we applied eight bursts of 1, 5 and 10  $\mu\text{s}$  long pulses ( $T_1$ ) with inter-phase delay of 0.5  $\mu\text{s}$  to 10 ms ( $T_2$ ) and an on-time of 800  $\mu\text{s}$ . We compared the effect of HF-EP to the standard ECT pulses, *i.e.* eight 100  $\mu\text{s}$  long pulses.

### 4.1. Monophasic vs HF-EP pulse treatment

We compared the efficiency of a monophasic and HF-EP pulse treatment in three different buffers. We determined that short biphasic pulses were less efficient in decreasing cell survival and increasing cell membrane permeability than monophasic pulses as es higher electric field had to be applied to achieve a similar effect (Figs. 2 and 3), which is in agreement with the existing HF-IRE and HF-EP studies [34,37,38,59].

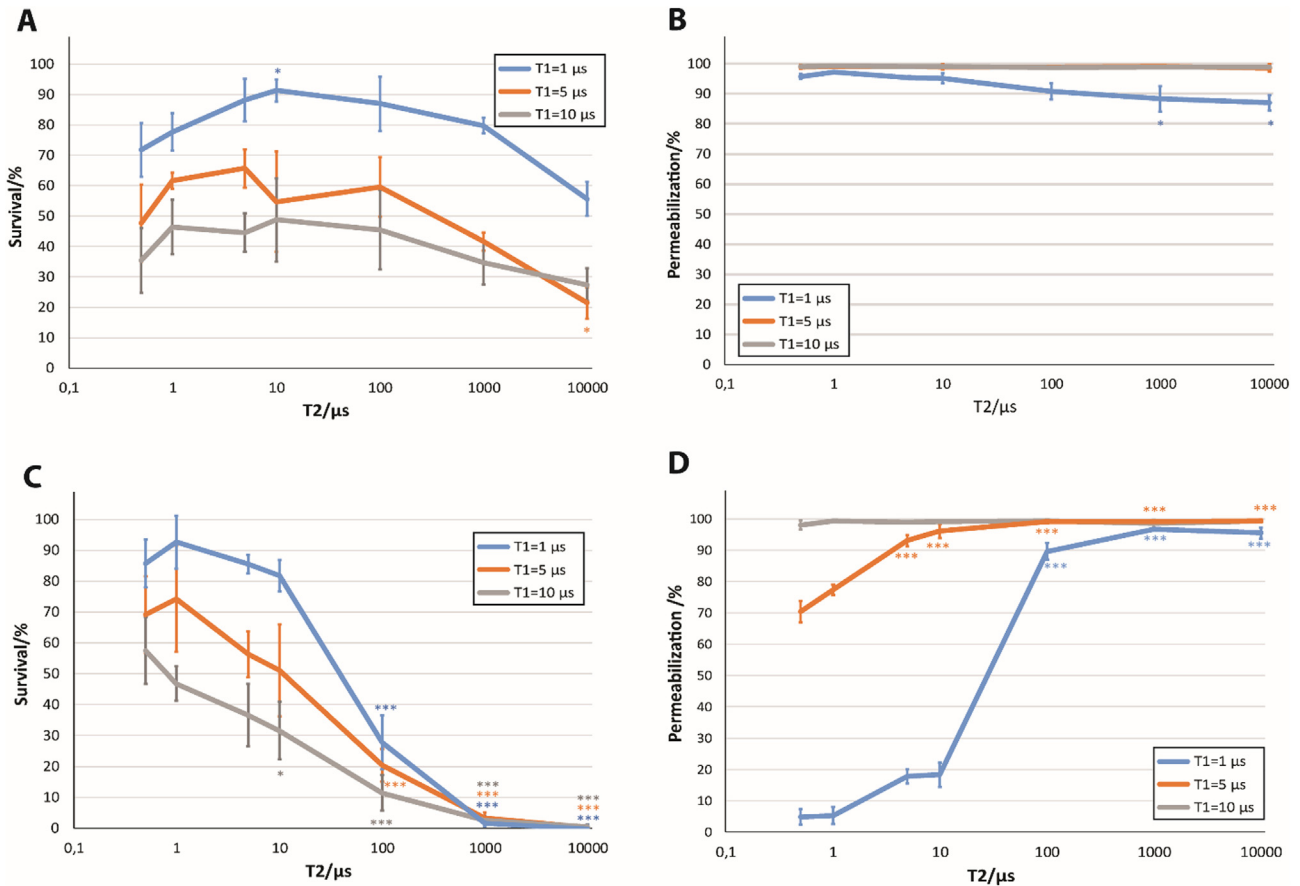


**Fig. 4.** Cancellation effect in survival and permeabilization after HF-EP pulse treatment in two different electroporation buffers as a function of pulse duration. In survival experiments, samples were exposed to 600 V (3000 V/cm) and in permeabilization experiments, to 320 V (1600 V/cm). Graphs A and B show results in low-conductivity buffer and graphs C and D in buffer 2 high-conductivity buffer. The asterisks (\*) mark  $p < 0.05^*$ ,  $p < 0.01^{**}$ ,  $p < 0.001^{***}$  and show statistically significant differences between  $T_2 = 0.5 \mu\text{s}$  (the shortest inter-phase delay) and  $\Delta T_2$ . Differences in each pulse length ( $T_1$ ) are shown in correspondent colors (blue  $1 \mu\text{s}$ , orange  $5 \mu\text{s}$  and gray  $10 \mu\text{s}$ ). (For interpretation of the references to color in this figure legend, the reader is referred to the web version of this article.)

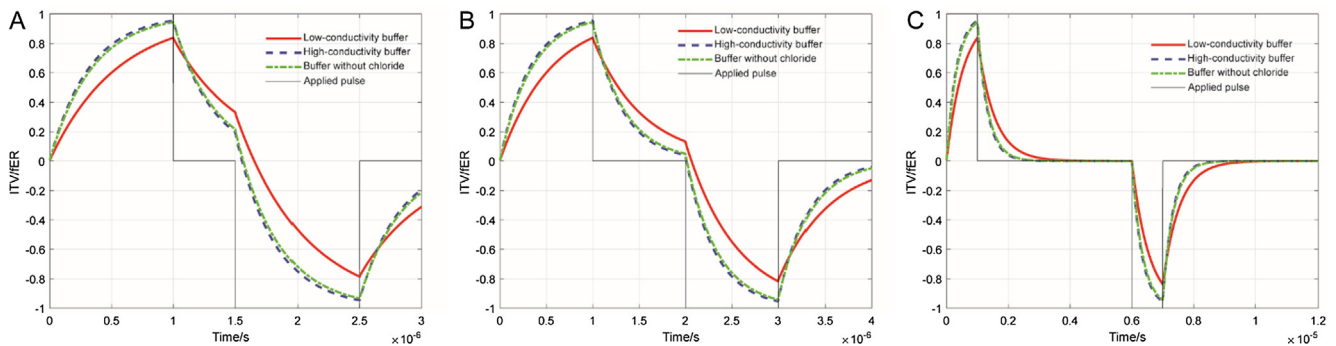


**Fig. 5.** Time constant of membrane charging as a function of the electric conductivity of the extracellular medium as a response to a step. We can see that in our experiments, time constant was in the range of  $0.3 \mu\text{s} - 0.5 \mu\text{s}$  for all three buffers. (A) The inter-phase delay was  $0.5 \mu\text{s}$  or  $1 \mu\text{s}$ . (C) The inter-phase delay of  $5 \mu\text{s}$  was already enough for membranes to completely discharge and for the negative pulse to be applied to a membrane at 0 V. Solid black line shows the shape of the applied biphasic pulse. The induced transmembrane voltage was normalized to geometrical factor  $f$ , applied electric field  $E$  and cell radius  $R$ . Red, blue and green lines show the normalized calculated time dependence of transmembrane voltage for low-conductivity, high-conductivity buffer and buffer without chloride, respectively. (For interpretation of the references to color in this figure legend, the reader is referred to the web version of this article.)

#### 4.2. Survival in HF-IRE pulse treatments

First, we focused on cell survival, as HF-IRE pulses are predominantly applied to obtain irreversible electroporation. We applied  $1 \mu\text{s}$  long pulses with two different inter-phase delays ( $1 \mu\text{s}$  and  $10 \mu\text{s}$ ) in three electroporation buffers as a function of the electric field. A cancellation effect was observed in all three buffers at a

high-enough electric field (from  $3 \text{ kV/cm}$  in the low-conductivity buffer, from  $1.5 \text{ kV/cm}$  in the high-conductivity buffer and the buffer without chloride) (Fig. 2) which is in agreement with already published studies where the cancellation effect was observed in assessing cell survival [46,49]. Interestingly, cells responded similarly in the high-conductivity buffer and the buffer without chloride; there was no significant difference at any of the tested

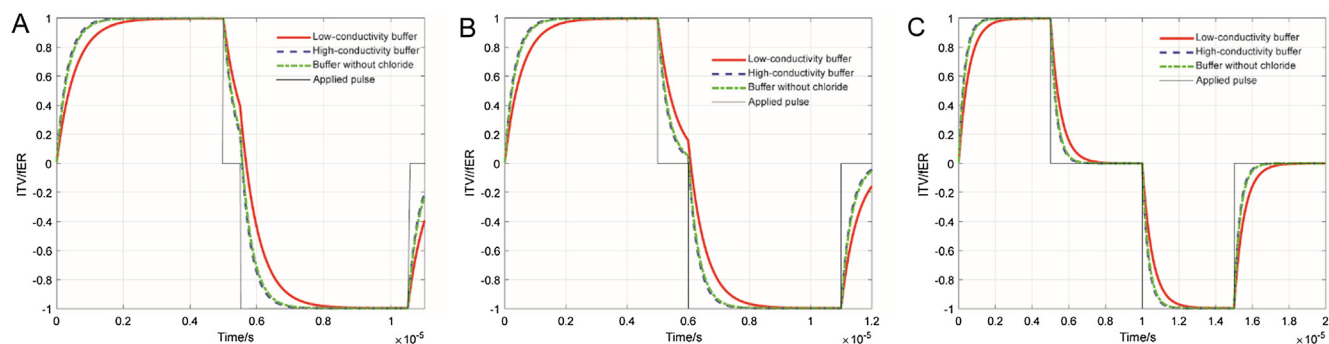


**Fig. 6.** Charging and discharging of the cell membrane when there is 1 0.5–5  $\mu\text{s}$  inter-phase delay between 5  $\mu\text{s}$  long pulses in three different electroperoration buffers. We can see that the stationary value of induced transmembrane value was reached during the pulse. (A) The inter-phase delay was 0.5  $\mu\text{s}$  or (B) 1  $\mu\text{s}$ . (C) The inter-phase delay of 5  $\mu\text{s}$  was already enough for membranes to completely discharge and for the negative pulse to be applied to a membrane at 0 V. Solid black line shows the shape of the applied biphasic pulse. The induced transmembrane voltage was normalized to geometrical factor  $f$ , applied electric field  $E$  and cell radius  $R$  [ $ITV/fER$ ]. Red, blue and green lines show the normalized calculated time dependence of transmembrane voltage for low-conductivity, high-conductivity buffer and buffer without chloride, respectively. (For interpretation of the references to color in this figure legend, the reader is referred to the web version of this article.)

**Table 4**  
Fraction of Induced transmembrane voltage normalized to geometric factor  $f$ , applied electric field  $E$  and cell radius  $R$  [ $ITV/fER$ ]. After the voltage is turned off, the transmembrane voltage decreases exponentially and depends on the time constant of the membrane, except when assisted ( $T_2 < 1 \mu\text{s}$ ).

	0.5 $\mu\text{s}$	1 $\mu\text{s}$	5 $\mu\text{s}$	10 $\mu\text{s}$	100 $\mu\text{s}$	1 ms	10 ms
Low-conductivity buffer	$3.97 \times 10^{-1}$	$1.58 \times 10^{-1}$	$9.74 \times 10^{-5}$	$9.49 \times 10^{-9}$	0	0	0
High-conductivity buffer	$2.05 \times 10^{-1}$	$4.21 \times 10^{-2}$	$1.32 \times 10^{-7}$	$1.75 \times 10^{-14}$	0	0	0
Buffer without chloride	$2.28 \times 10^{-1}$	$5.21 \times 10^{-2}$	$3.85 \times 10^{-7}$	$1.48 \times 10^{-13}$	0	0	0

electric fields which indicates that extracellular chloride ions do not play a major role in cell survival after electroperoration.

In Fig. 4, a wider range of inter-phase delays was tested at a fixed electric field (3 kV/cm). In the low-conductivity buffer, no cancellation effect was observed when we compared different  $T_2$  to the shortest  $T_2 = 0.5 \mu\text{s}$  used. A statistically significant difference between  $T_2 = 1 \mu\text{s}$  and  $T_2 = 10 \text{ms}$  was observed, as seen in Fig. 2 and also in Fig. 4 ( $p < 0.05$ ). In the high-conductivity buffer, cell survival increased with decreasing inter-phase delay, i.e. the cancellation effect was observed. With longer pulses (10  $\mu\text{s}$ ), lower electric fields were already sufficient to achieve a similar decrease in cell survival than with shorter pulses (1  $\mu\text{s}$ ), regardless of the chosen buffer and the inter-phase delay (Figs. 2 and 4), which is in agreement with existing studies on the electroperoration strength-duration curve [60]. Thus, longer pulses than 1  $\mu\text{s}$  could be applied in HF-IRE treatments to increase efficiency; however, the suggested benefit of reducing pain and muscle contractions at longer pulses would need to be reevaluated.

#### 4.3. Permeabilization in HF-EP pulse treatment

We expected the results in permeabilization experiments to be similar to the ones in survival experiments, as survival and permeability are believed to be correlated, and increased permeabilization is a prerequisite for possible cell death [11]. First, we focused on 1  $\mu\text{s}$  long pulses with 1  $\mu\text{s}$  and 10 ms inter-phase delay as a function of the electric field in three electroperoration buffers. Unexpectedly, in the low-conductivity buffer, permeabilization was more efficient with 1  $\mu\text{s}$  than with 10 ms inter-phase delay, i.e., we observed a reversed cancellation effect, opposite to our expectations and the existing literature [49]. Although cells responded very similarly in the low- and the high-conductivity buffers with the 10 ms inter-phase delay, they responded oppositely with the 1  $\mu\text{s}$  inter-phase delay, thus indicating that the phenomenon causing cancellation effect happens in the time-range of 1  $\mu\text{s}$  to 10 ms, as already reported for ns pulses [49,50].

Translation of results from *in vitro* to *in vivo* thus seems not to be straightforward and/or is even questionable. When inferring the *in vivo* response from the *in vitro* experiments, the importance of electroperoration buffer should be taken into account, and perhaps, the buffer most similar to tissues should be used. In this paper we consider this to be the high-conductivity buffer, due to the presence of NaCl.

In Fig. 4, a wider range of inter-phase delays at 1600 V/cm was tested. We wanted to determine if in the low-conductivity buffer, the reversed cancellation effect was present also with other inter-phase and pulse lengths. However, it was mostly observed for the pulse length of 1  $\mu\text{s}$ . Longer pulses mostly caused complete cell membrane permeabilization, and we could not distinguish between the effects of different inter-phase delays. The cancellation effect was however observed in high-conductivity buffer and it depends on pulse length.

Electroperoration can be induced also by exposure of cells to pulse modulated sine wave signals [61]. The efficiency of treatment decreased when frequency of sinewaves was increased [59]. This is comparable to the efficiency of HF-EP: biphasic pulses with longer (10 ms) inter-phase delay are more effective in permeabilizing cells than biphasic pulses with short (1  $\mu\text{s}$ ) inter-phase delay (Fig. 2). In HF-EP pulse treatment this happens due to cancellation effect. This may be partly explained by the fact that at longer interphase delays, relatively more power is delivered at the lower frequency range of the signal.

#### 4.4. Effect of electroperoration buffers

It was already shown that electroperoration buffer has a significant effect on the cell membrane permeabilization *in vitro* [57]. Thus, we used three different electroperoration buffers: the low-conductivity potassium-phosphate buffer, usually used in many laboratories, the high-conductivity buffer where sucrose was substituted with NaCl in an iso-osmolar manner and the buffer without chloride. Interestingly, it was previously observed that in *in vitro* permeability experiments, cells responded very differently

when electroporated in the low- or high-conductivity buffers in the time-range of minutes, in the experiments on the so-called 'cell sensitization' [57]. Here, a parallel can be drawn as we also observed very different responses in the same buffers (Fig. 4).

In permeability experiments, it was observed that the cancellation effect was more pronounced in the low-conductivity buffers than in the high-conductivity buffers with no or very short inter-pulse intervals [51]. However, our results contradict these results, as the cancellation effect was not observed in the low-conductivity buffer; moreover, the 'sensitization' effect was observed. In our experiments, the cancellation was observed in the high-conductivity and medium-conductivity buffers (*i.e.* buffer without chloride), but not in the low-conductivity buffer. It is possible that low conductivity caused the lack of cancellation effect, although it is more possible that the high sucrose concentration was responsible, similarly, as indicated in [57].

#### 4.4.1. Contribution of chloride channels

Since the absence of muscle contraction using HF-IRE pulses was also demonstrated [31,33,34,36,59,62–66], we assumed that HF-EP pulse treatment inhibits the induction of action potentials. Fast reversal of pulse polarities causes a reversal in depolarization and hyperpolarization of the membrane. One of the hyperpolarization-activated inward currents is produced by the chloride ions [67,68]. Opening of the  $\text{Cl}^-$  channels can be activated in the presence of  $\text{Cl}^-$  ions. The influx of  $\text{Cl}^-$  ions after the first pulse would decrease the resting potential, cause hyperpolarization and make it more difficult for excitable cells to reach membrane potential required for activation of the action potential, thus, abolishing the action potential. Similarly, due to the lower resting membrane potential, a higher electric field would need to be applied to reach the same transmembrane voltage as without the influx of chloride ions, making cells less sensitive to the following pulses, *i.e.* causing the cancellation effect. The activation time constant of voltage-gated  $\text{Cl}^-$  ion channels in skeletal muscle comprises two components, a fast gate ( $\sim 16 \mu\text{s}$ ) and a slow gate ( $\sim 1 \text{ms}$ ) [56], which could explain the influence of the inter-phase delay T2 on the cell membrane permeabilization and cell death. Voltage-gated chloride channels are known to be present in CHO cells [69]. Thus, we tested this theory by preparing a buffer without chloride ions. Elimination of the cancellation effect was expected, yet the cancellation effect was present. Thus, our hypothesis on the contribution of the chloride channels to the cancellation effect was dismissed.

#### 4.5. Temperature effect

Temperature has a significant effect on the efficiency of electroporation, *e.g.* it was shown that changes in temperature affect gene electrotransfer [70,71], cell membrane permeabilization [72], skin electroporation [73] and breakdown voltage of lipid bilayers [74]. Moreover, electric pulses cause Joule heating and consequently, they can cause thermal damage [75,76]. The threshold for thermal damage is  $42^\circ\text{C}$  for prolonged exposure, while the temperature should not exceed  $50^\circ\text{C}$  at any time [77]. In our experiments, at applications of 1000 V the temperature increased up to  $45^\circ\text{C}$  from the room temperature ( $24^\circ\text{C}$ ), *i.e.* it increased for  $22^\circ\text{C}$  and thermal damage was obtained. Between different tissues, the electric conductivity varies significantly and is generally in the range of  $10^{-2}$  to  $2 \text{S/m}$  [78,79] which is a similar range as the conductivities of the buffers in our study ( $0.1\text{--}2 \text{S/m}$ ). Considering that in tissues the initial temperature is around  $37^\circ\text{C}$ , we can expect thermal damage predominantly around the electrodes due to high current density and at very high electric fields, longer pulse lengths and shorter inter-phase delays.

When 600 V was delivered to buffers, the temperature changed for approx.  $7^\circ\text{C}$  at all pulse lengths ( $T1 = 1, 5$  and  $10 \mu\text{s}$ ) (Table S1). Survival experiments performed at the same condition showed different cancellation effect (Fig. 4c), therefore we can assume cancellation effect is not effected by the temperature but by the pulse parameters.

#### 4.6. Effect of the assisted discharge

Several hypotheses were put forth to explain the cancellation effect, but so far none could completely explain the phenomenon. We focused on the assisted discharge, as the three buffers we used varied vastly in their electric conductivity. In survival assays, cells electroporated in the high-conductivity buffer and buffer without chloride were more sensitive than those in the low-conductivity buffer when the inter-phase delay was  $1 \mu\text{s}$  (Fig. 2). Incomplete membrane charging and assisted membrane discharge [49] lend themselves as a plausible explanation for such behavior. In permeabilization assays, cells were generally the most sensitive to electroporation in the low-conductivity buffer (Fig. 3). As in the high-conductivity buffer and the buffer without chloride the charging was faster than in the low-conductivity buffer (Fig. 6), we cannot explain less permeabilization in the high-conductivity buffer and in the buffer without chloride than in low-conductivity buffer with the difference in membrane charging. The assisted discharge influences results up to  $1.5 \mu\text{s}$  for the high-conductivity buffer and the buffer without calcium, and  $2.5 \mu\text{s}$  in the low-conductivity buffer after voltage is turned on (Fig. 6). This means that permeabilization should be more efficient with the  $10 \text{ms}$  inter-phase delay than with the  $1 \mu\text{s}$  in all buffers, which is true for cell survival but not for cell membrane permeabilization. We can thus conclude that the time constant of membrane charging, together with the assisted discharge, could only partially explain the discrepancies in the experimental data.

#### 4.7. Drawbacks of our study

We applied bursts of biphasic pulses, while in studies on cancellation effects single biphasic pulses or single trains were applied. Thus, it is possible that because our pulse application lasted for 8 s, additional effects were present [80].

It is possible that by applying different voltages in Fig. 4, or even adapting the voltages to separate electroporation buffers, the presence of a cancellation effect would be more clear. However, we decided to fix the voltage to be able to compare the results at the same electric field.

In the theoretical calculation of the assisted discharge as a function of extracellular conductivity, we assumed that all cells in the suspension are of the same size, which is a simplification [81]. The size of the radii namely follows the Gaussian distribution which means that also time constants of the membrane are statistically distributed vary through the population.

In temperature measurements, we aimed to measure the temperature always at the same spot in the cell suspension. However, due to the limited precision of positioning the probe, its position could slightly vary between the treatments. Also, we measured the macroscopic increase in temperature. It was previously shown that even when the macroscopic increase is negligible, at the cell level, there could still be some thermal damage in intermediate vicinity of the electrodes [82,83].

## 5. Conclusion

In our study, we focused on the previously reported cancellation effects in *in vitro* electroporation with bursts of short biphasic

pulses. The following main conclusions can be drawn from our work. (1) Cancellation effect is present in HF-EP treatments looking at survival and could be responsible for the need to apply higher electric fields in HF-IRE treatments than in IRE treatments. (2) Cancellation effect is present in a wide range of pulse parameters and depends on the inter-phase delay as well as on pulse duration, *i.e.* cancellation is less pronounced with longer pulses and longer interphase delays. (3) Cancellation effect is electroporation-buffer dependent. (4) Cancellation effect in survival experiments can be only partially explained by the assisted discharge. (5) Cancellation effect is not caused by the hyperpolarization.

#### Author contribution

- Tamara Polajžer: acquisition of the data, analysis and interpretation of the data, drafting the paper, final approval of the paper.
- Janja Dermol-Černe: analysis and interpretation of the data, drafting the paper, final approval of the paper.
- Matej Reberšek: design of the ns- $\mu$ s pulse generator, used in the study, final approval of the paper.
- Rodney O'Connor: conception and design of the study, final approval of the paper.
- Damijan Miklavčič: conception and design of the study, analysis and interpretation of the data, drafting the paper, final approval of the paper.

#### Declaration of Competing Interest

The authors declare that they have no known competing financial interests or personal relationships that could have appeared to influence the work reported in this paper.

#### Acknowledgements

The authors acknowledge the financial support from the Slovenian Research Agency (research core funding No. IP-0510 and P2-0249). The research was conducted within the scope of the European Associated Laboratory on the Electroporation in Biology and Medicine (LEA-EBAM). The authors would like to thank Dr M. Bešter-Rogač from the Faculty of Chemistry and Chemical Technology, University of Ljubljana for the help with osmolality measurements. Authors would like to thank Dr M. Kranjc for his help with temperature measurements and L. Vukanović and D. Hodžič for their help in the cell culture laboratory.

#### References

- [1] T. Kotnik, L. Rems, M. Tarek, D. Miklavčič, Membrane electroporation and electroporation: mechanisms and models, *Annu. Rev. Biophys.* (2019), <https://doi.org/10.1146/annurev-biophys-052118-115451>.
- [2] D. Miklavčič et al., Electrochemotherapy: technological advancements for efficient electroporation-based treatment of internal tumors, *Med. Biol. Eng. Comput.* 50 (12) (2012) 1213–1225, <https://doi.org/10.1007/s11517-012-0991-8>.
- [3] D. Miklavčič, B. Mali, B. Kos, R. Heller, G. Serša, Electrochemotherapy: from the drawing board into medical practice Electrochemotherapy for skin and superficial tumors, *Electrochemotherapy for visceral and deep-seated tumors*, *Biomed. Eng.* 13 (2014) 1–20, <https://doi.org/10.1186/1475-925X-13-29>.
- [4] J. Gehl et al., Updated standard operating procedures for electrochemotherapy of cutaneous tumours and skin metastases, *Acta Oncol.* 57 (7) (2018) 874–882, <https://doi.org/10.1080/0284186X.2018.1454602>.
- [5] L.G. Campana et al., Electrochemotherapy of superficial tumors – Current status: Basic principles, operating procedures, shared indications, and emerging applications, *Semin. Oncol.* (2019), <https://doi.org/10.1053/j.seminoncol.2019.04.002>.
- [6] L.C. Heller, R. Heller, *Electroporation gene therapy preclinical and clinical trials for melanoma*, *Curr. Gene Ther.* 10 (4) (2010) 312–317.
- [7] L. Lambricht, A. Lopes, S. Kos, G. Sersa, V. Prát, G. Vandermeulen, Clinical potential of electroporation for gene therapy and DNA vaccine delivery, *Expert Opin. Drug Deliv.* 13 (2) (2016) 295–310, <https://doi.org/10.1517/17425247.2016.1121990>.
- [8] C.L. Trimble et al., Safety, efficacy, and immunogenicity of VGX-3100, a therapeutic synthetic DNA vaccine targeting human papillomavirus 16 and 18 E6 and E7 proteins for cervical intraepithelial neoplasia 2/3: a randomised, double-blind, placebo-controlled phase 2b trial, *Lancet (London, England)* 386 (10008) (2015) 2078–2088, [https://doi.org/10.1016/S0140-6736\(15\)00239-1](https://doi.org/10.1016/S0140-6736(15)00239-1).
- [9] K. Kwak et al., Multivalent human papillomavirus L1 DNA vaccination utilizing electroporation, *PLoS One* (2013), <https://doi.org/10.1371/journal.pone.0060507>.
- [10] H.J. Scheffer et al., Irreversible electroporation for nonthermal tumor ablation in the clinical setting: a systematic review of safety and efficacy, *J. Vasc. Interv. Radiol.* 25 (7) (2014) 997–1011, <https://doi.org/10.1016/j.jvir.2014.01.028>.
- [11] C. Jiang, R.V. Davalos, J.C. Bischof, A review of basic to clinical studies of irreversible electroporation therapy, *IEEE Trans. Biomed. Eng.* 62 (1) (2015) 4–20, <https://doi.org/10.1109/TBME.2014.2367543>.
- [12] A. Wojtaszczyk, G. Caluori, M. Pešl, K. Melajova, Z. Stárek, Irreversible electroporation ablation for atrial fibrillation, *J. Cardiovasc. Electrophysiol.* 29 (4) (2018) 643–651, <https://doi.org/10.1111/jce.13454>.
- [13] V.Y. Reddy et al., Pulsed field ablation for pulmonary vein isolation in atrial fibrillation, *J. Am. Coll. Cardiol.* (2019), <https://doi.org/10.1016/j.jacc.2019.04.021>.
- [14] F.H.M. Wittkamp, R. van Es, K. Neven, Electroporation and its relevance for cardiac catheter ablation, *JACC. Clin. Electrophysiol.* 4 (8) (2018) 977–986, <https://doi.org/10.1016/j.jacep.2018.06.005>.
- [15] M.T. Stewart et al., Intracardiac pulsed field ablation: proof of feasibility in a chronic porcine model, *Hear. Rhythm* (2019), <https://doi.org/10.1016/j.hrthm.2018.10.030>.
- [16] S. Mahnič-Kalamiza, E. Vorobiev, D. Miklavčič, Electroporation in food processing and biorefinery, *J. Membr. Biol.* 247 (12) (2014) 1279–1304, <https://doi.org/10.1007/s00232-014-9737-x>.
- [17] T. Kotnik, W. Frey, M. Sack, S. Haberl Meglič, M. Peterka, D. Miklavčič, Electroporation-based applications in biotechnology, *Trends Biotechnol.* 33 (8) (2015) 480–488, <https://doi.org/10.1016/j.tibtech.2015.06.002>.
- [18] A. Golberg et al., Energy-efficient biomass processing with pulsed electric fields for bioeconomy and sustainable development, *Biotechnol. Biofuels* (2016), <https://doi.org/10.1186/s13068-016-0508-z>.
- [19] S. Toepfl, C. Siemer, G. Saldaña-Navarro, V. Heinz, Chapter 6 – Overview of pulsed electric fields processing for food, *Emerg. Technol. Food Process.* (2014), <https://doi.org/10.1016/B978-0-12-411479-1.00006-1>.
- [20] M. Marty et al., Electrochemotherapy – An easy, highly effective and safe treatment of cutaneous and subcutaneous metastases: results of ESOPE (European Standard Operating Procedures of Electrochemotherapy) study, *Eur. J. Cancer, Suppl.* (2006), <https://doi.org/10.1016/j.ejcsup.2006.08.002>.
- [21] D. Miklavcic, S. Corovic, G. Pucihar, N. Pavselj, Importance of tumour coverage by sufficiently high local electric field for effective electrochemotherapy, *Eur. J. Cancer Suppl.* 4 (11) (2006) 45–51, <https://doi.org/10.1016/J.EJCSUP.2006.08.006>.
- [22] C.B. Arena, R.V. Davalos, Advances in therapeutic electroporation to mitigate muscle contractions, *J. Membr. Sci. Technol.* 02 (01) (2012) 1–3, <https://doi.org/10.4172/2155-9589.1000e102>.
- [23] A. Zupanic, S. Ribaric, D. Miklavcic, Increasing the repetition frequency of electric pulse delivery reduces unpleasant sensations that occur in electrochemotherapy, *Neoplasma* 54 (3) (2007) 246–250.
- [24] R.C. Martin, E. Schwartz, J. Adams, I. Farah, B.M. Derhake, Intra-operative anesthesia management in patients undergoing surgical irreversible electroporation of the pancreas, liver, kidney, and retroperitoneal tumors, *Anesthesiol. Pain Med.* (2015), <https://doi.org/10.5812/aapm.22786>.
- [25] B. Mali et al., The effect of electroporation pulses on functioning of the heart, *Med. Biol. Eng. Comput.* (2008), <https://doi.org/10.1007/s11517-008-0346-7>.
- [26] B. Mali et al., Electrochemotherapy of colorectal liver metastases – an observational study of its effects on the electrocardiogram, *Biomed. Eng.* 14 (Suppl. 3) (2015) S5, <https://doi.org/10.1186/1475-925X-14-S3-S5>.
- [27] C. Ball, K.R. Thomson, H. Kavnoudias, Irreversible electroporation, *Anesth. Analg.* 110 (5) (2010) 1305–1309, <https://doi.org/10.1213/ANE.0b013e3181d27b30>.
- [28] D. Miklavčič et al., The effect of high frequency electric pulses on muscle contractions and antitumor efficiency in vivo for a potential use in clinical electrochemotherapy, *Bioelectrochemistry* 65 (2) (2005) 121–128.
- [29] G. Pucihar, L.M. Mir, D. Miklavcic, The effect of pulse repetition frequency on the uptake into electroporation-based cells in vitro with possible applications in electrochemotherapy, *Bioelectrochemistry* 57 (2) (2002) 167–172.
- [30] G. Sersa, S. Kranjc, J. Scancar, M. Krzan, M. Cemazar, Electrochemotherapy of mouse sarcoma tumors using electric pulse trains with repetition frequencies of 1 Hz and 5 kHz, *J. Membr. Biol.* (2010), <https://doi.org/10.1007/s00232-010-9268-z>.
- [31] C. Yao et al., Bipolar microsecond pulses and insulated needle electrodes for reducing muscle contractions during irreversible electroporation, *IEEE Trans. Biomed. Eng.* 64 (12) (2017) 2924–2937, <https://doi.org/10.1109/TBME.2017.2690624>.
- [32] A. Golberg, B. Rubinsky, Towards electroporation based treatment planning considering electric field induced muscle contractions, *Technol. Cancer Res. Treat.* (2013), <https://doi.org/10.7785/tcrt.2012.500249>.
- [33] C.B. Arena et al., High-frequency irreversible electroporation (H-FIRE) for non-thermal ablation without muscle contraction, *Biomed. Eng.* 10 (1) (2011) 102, <https://doi.org/10.1186/1475-925X-10-102>.
- [34] Y. Zhao et al., Characterization of conductivity changes during high-frequency irreversible electroporation for treatment planning, *IEEE Trans. Biomed. Eng.* (2018), <https://doi.org/10.1109/TBME.2017.2778101>.

- [35] M.B. Sano et al., Bursts of bipolar microsecond pulses inhibit tumor growth, *Sci. Rep.* 5 (2015) 14999, <https://doi.org/10.1038/srep14999>.
- [36] S. Dong, H. Wang, Y. Zhao, Y. Sun, C. Yao, First human trial of high-frequency irreversible electroporation therapy for prostate cancer, *Technol. Cancer Res. Treat.* (2018), <https://doi.org/10.1177/1533033818789692>.
- [37] D.C. Sweeney, M. Reberšek, J. Dermol, L. Rems, D. Miklavčič, R.V. Davalos, Quantification of cell membrane permeability induced by monopolar and high-frequency bipolar bursts of electrical pulses, *Biochim. Biophys. Acta - Biomembr.* 1858 (11) (2016) 2689–2698, <https://doi.org/10.1016/j.bbame.2016.06.024>.
- [38] M. Scuderi, M. Reberšek, D. Miklavčič, J. Dermol-Cerne, The use of high-frequency short bipolar pulses in cisplatin electrochemotherapy in vitro, *Radiol. Oncol.* 53 (2) (2019) 194–205, <https://doi.org/10.2478/raon-2019-0025>.
- [39] E. Tekle, R.D. Astumiant, P. Boon Chock, Electroporation by using bipolar oscillating electric field: an improved method for DNA transfection of NIH 3T3 cells, *Biochemistry* 88 (1991) 4230–4234.
- [40] T. Kotnik, L.M. Mir, K. Flisar, M. Puc, D. Miklavčič, Cell membrane electroporation by symmetrical bipolar rectangular pulses: part I. Increased efficiency of permeabilization, *Bioelectrochemistry* 54 (1) (2001) 83–90, [https://doi.org/10.1016/S1567-5394\(01\)00114-1](https://doi.org/10.1016/S1567-5394(01)00114-1).
- [41] T. Kotnik, D. Miklavčič, L.M. Mir, Cell membrane electroporation by symmetrical bipolar rectangular pulses: part II. Reduced electrolytic contamination, *Bioelectrochemistry* 54 (1) (2001) 91–95, [https://doi.org/10.1016/S1567-5394\(01\)00115-3](https://doi.org/10.1016/S1567-5394(01)00115-3).
- [42] I. Daskalov, N. Mudrov, E. Peycheva, Exploring new instrumentation parameters for electrochemotherapy. Attacking tumors with bursts of biphasic pulses instead of single pulses, *IEEE Eng. Med. Biol. Mag.* 18 (1), 62–66.
- [43] S. Jaichandran, S.T.B. Yap, A.B.M. Khoo, L.P. Ho, S.L. Tien, O.L. Kon, In vivo liver electroporation: optimization and demonstration of therapeutic efficacy, *Hum. Gene Ther.* 17 (3) (2006) 362–375, <https://doi.org/10.1089/hum.2006.17.362>.
- [44] L. Pasquet et al., Safe and efficient novel approach for non-invasive gene electrotransfer to skin, *Sci. Rep.* (2018), <https://doi.org/10.1038/s41598-018-34968-6>.
- [45] M. Reberšek, D. Miklavčič, C. Bertacchini, M. Sack, Cell membrane electroporation-Part 3: the equipment, *IEEE Electr. Insul. Mag.* (2014), <https://doi.org/10.1109/MEI.2014.6804737>.
- [46] B.L. Ibey et al., Bipolar nanosecond electric pulses are less efficient at electroporation and killing cells than monopolar pulses, *Biochem. Biophys. Res. Commun.* 443 (2) (2014) 568–573, <https://doi.org/10.1016/j.bbrc.2013.12.004>.
- [47] A.G. Pakhomov, S. Grigoryev, I. Semenov, M. Casciola, C. Jiang, S. Xiao, The second phase of bipolar, nanosecond-range electric pulses determines the electroporation efficiency, *Bioelectrochemistry* 122 (2018) 123–133, <https://doi.org/10.1016/j.bioelechem.2018.03.014>.
- [48] C.M. Valdez, R.A. Barnes, C.C. Roth, E.K. Moen, G.A. Throckmorton, B.L. Ibey, Asymmetrical bipolar nanosecond electric pulse widths modify bipolar cancellation, *Sci. Rep.* (2017), <https://doi.org/10.1038/s41598-017-16142-6>.
- [49] A.G. Pakhomov et al., Cancellation of cellular responses to nanosecond electroporation by reversing the stimulus polarity, *Cell. Mol. Life Sci.* 71 (22) (2014) 4431–4441, <https://doi.org/10.1007/s00018-014-1626-z>.
- [50] C.M. Valdez, R. Barnes, C.C. Roth, E. Moen, B. Ibey, The interphase interval within a bipolar nanosecond electric pulse modulates bipolar cancellation, *Bioelectromagnetics* 39 (6) (2018) 441–450, <https://doi.org/10.1002/bem.22134>.
- [51] E.C. Gianulis, M. Casciola, S. Xiao, O.N. Pakhomova, A.G. Pakhomov, Electroporation by uni- or bipolar nanosecond electric pulses: the impact of extracellular conductivity, *Bioelectrochemistry* 119 (2018) 10–19, <https://doi.org/10.1016/j.bioelechem.2017.08.005>.
- [52] T.R. Gowrishankar, J.V. Stern, K.C. Smith, J.C. Weaver, Nanopore occlusion: a biophysical mechanism for bipolar cancellation in cell membranes, *Biochem. Biophys. Res. Commun.* (2018), <https://doi.org/10.1016/j.bbrc.2018.07.024>.
- [53] C. Merla, A.G. Pakhomov, I. Semenov, P.T. Vernier, Frequency spectrum of induced transmembrane potential and permeabilization efficacy of bipolar electric pulses, *Biochim. Biophys. Acta Biomembr.* 1859 (7) (2017) 1282–1290, <https://doi.org/10.1016/j.bbame.2017.04.014>.
- [54] D. Shamon et al., Assessing the electro-deformation and electro-poration of biological cells using a three-dimensional finite element model, *Appl. Phys. Lett.* (2019), <https://doi.org/10.1063/1.5079292>.
- [55] T.J. Jentsch, V. Stein, F. Weinreich, A.A. Zdebik, Molecular structure and physiological function of chloride channels, *Physiol. Rev.* 82 (2) (2002) 503–568, <https://doi.org/10.1152/physrev.00029.2001>.
- [56] A. Accardi, M. Pusch, Fast and slow gating relaxations in the muscle chloride channel CLC-1, *J. Gen. Physiol.* (2000).
- [57] J. Dermol, O.N. Pakhomova, A.G. Pakhomov, D. Miklavčič, Cell electrosensitization exists only in certain electroporation buffers, *10.1371/journal.pone.0159434*.
- [58] T. Kotnik, D. Miklavčič, T. Slivnik, Time course of transmembrane voltage induced by time-varying electric fields - A method for theoretical analysis and its application, *Bioelectrochem. Bioenerg.* 45 (1) (1998) 3–16, [https://doi.org/10.1016/S0302-4598\(97\)00093-7](https://doi.org/10.1016/S0302-4598(97)00093-7).
- [59] S. Dong, C. Yao, Y. Zhao, Y. Lv, H. Liu, Parameters optimization of bipolar high frequency pulses on tissue ablation and inhibiting muscle contraction, *IEEE Trans. Dielectr. Electr. Insul.* (2018), <https://doi.org/10.1109/TDEI.2018.006303>.
- [60] G. Pucihar, J. Krmelj, M. Reberšek, T.B. Napotnik, D. Miklavčič, Equivalent pulse parameters for electroporation, *IEEE Trans. Biomed. Eng.* 58 (11) (2011) 3279–3288, <https://doi.org/10.1109/TBME.2011.2167232>.
- [61] T. Kotnik, G. Pucihar, M. Reberšek, D. Miklavčič, L.M. Mir, Role of pulse shape in cell membrane electroporation, *Biochim. Biophys. Acta - Biomembr.* 1614 (2) (2003) 193–200, [https://doi.org/10.1016/S0005-2736\(03\)00173-1](https://doi.org/10.1016/S0005-2736(03)00173-1).
- [62] C.B. Arena et al., Focal blood-brain-barrier disruption with high-frequency pulsed electric fields, *Technology* (2014), <https://doi.org/10.1142/s2339547814500186>.
- [63] I.A. Siddiqui et al., Induction of rapid, reproducible hepatic ablations using next-generation, high frequency irreversible electroporation (H-FIRE) in vivo, *HPB (Oxford)* 18 (9) (2016) 726–734, <https://doi.org/10.1016/j.hpb.2016.06.015>.
- [64] M.B. Sano et al., Reduction of muscle contractions during irreversible electroporation therapy using high-frequency bursts of alternating polarity pulses: a laboratory investigation in an ex vivo swine model, *J. Vasc. Interv. Radiol.* 29 (6) (2018) 893–898, <https://doi.org/10.1016/j.jvir.2017.12.019>.
- [65] B. Mercadal, C.B. Arena, R.V. Davalos, A. Ivorra, Avoiding nerve stimulation in irreversible electroporation: a numerical modeling study, *Phys. Med. Biol.* 62 (20) (2017) 8060–8079, <https://doi.org/10.1088/1361-6560/aa8c53>.
- [66] V.M. Ringel-Scaia et al., High-frequency irreversible electroporation is an effective tumor ablation strategy that induces immunologic cell death and promotes systemic anti-tumor immunity, *EBioMedicine* 44 (Jun. 2019) 112–125, <https://doi.org/10.1016/j.ebiom.2019.05.036>.
- [67] S. Clark, S.E. Jordt, T.J. Jentsch, A. Mathie, Characterization of the hyperpolarization-activated chloride current in dissociated rat sympathetic neurons, *J. Physiol.* 506 (Pt 3) (1998) 665–678, <https://doi.org/10.1111/j.1469-7793.1998.665BV.x>.
- [68] M. Pusch, S.E. Jordt, V. Stein, T.J. Jentsch, Chloride dependence of hyperpolarization-activated chloride channel gates, *J. Physiol.* 515 (Pt 2) (1999) 341–353, <https://doi.org/10.1111/j.1469-7793.1999.341AC.x>.
- [69] X. Li, K. Shimada, L.A. Showalter, S.A. Weinman, Biophysical properties of CLC-3 differentiate it from swelling-activated chloride channels in Chinese hamster ovary-K1 cells, *J. Biol. Chem.* (2000), <https://doi.org/10.1074/jbc.M002712200>.
- [70] M. Pierre Rols, C. Delteil, G. Serin, J. Teissié, Temperature effects on electrotransfection of mammalian cells, *Nucleic Acids Res.* (1994), <https://doi.org/10.1093/nar/22.3.540>.
- [71] A. Bulysheva et al., Coalesced thermal and electrotransfer mediated delivery of plasmid DNA to the skin, *Bioelectrochemistry* (2019), <https://doi.org/10.1016/j.bioelechem.2018.10.004>.
- [72] M. Kandušer, M. Šentjurc, D. Miklavčič, The temperature effect during pulse application on cell membrane fluidity and permeabilization, *Bioelectrochemistry* (2008), <https://doi.org/10.1016/j.bioelechem.2008.04.012>.
- [73] U.F. Pliquett, G.T. Martin, J.C. Weaver, Kinetics of the temperature rise within human stratum corneum during electroporation and pulsed high-voltage iontophoresis, *Bioelectrochemistry* 57 (1) (2002) 65–72.
- [74] A. Velikonja, P. Kramar, D. Miklavčič, A. Maček Lebar, Specific electrical capacitance and voltage breakdown as a function of temperature for different planar lipid bilayers, *Bioelectrochemistry* 112 (2016) 132–137, <https://doi.org/10.1016/j.bioelechem.2016.02.009>.
- [75] M. Faroja et al., Irreversible electroporation ablation: is all the damage nonthermal?, *Radiology* (2012), <https://doi.org/10.1148/radiol.12120609>.
- [76] Long, Histological and finite element analysis of cell death due to irreversible electroporation, *TCRT Exp.* (2013), <https://doi.org/10.7785/TCRTExp.2013.600253>.
- [77] R.V. Davalos, B. Rubinsky, L.M. Mir, Theoretical analysis of the thermal effects during in vivo tissue electroporation, *Bioelectrochemistry* 61 (1–2) (2003) 99–107.
- [78] S. Gabriel, R.W. Lau, C. Gabriel, The dielectric properties of biological tissues: II. Measurements in the frequency range 10 Hz to 20 GHz, *Phys. Med. Biol.* (1996), <https://doi.org/10.1088/0031-9155/41/11/002>.
- [79] IT'IS Foundation, Tissue Properties Database V4.0. IT'IS Foundation, 2018, 10.13099/VIP21000-04-0.
- [80] O.N. Pakhomova, B.W. Gregory, V.A. Khorokhorina, A.M. Bowman, S. Xiao, A.G. Pakhomov, Electroporation-induced electrosensitization, *PLoS One* 6 (2) (2011), <https://doi.org/10.1371/journal.pone.0017100>.
- [81] M. Puc, T. Kotnik, L.M. Mir, D. Miklavčič, Quantitative model of small molecules uptake after in vitro cell electroporation, *Bioelectrochemistry* 60 (1–2) (2003) 1–10.
- [82] T. Kotnik, D. Miklavčič, Theoretical evaluation of the distributed power dissipation in biological cells exposed to electric fields, *Bioelectromagnetics* 21 (5) (2000) 385–394.
- [83] P.A. García, R.V. Davalos, D. Miklavčič, A numerical investigation of the electric and thermal cell kill distributions in electroporation-based therapies in tissue, *PLoS One* (2014), <https://doi.org/10.1371/journal.pone.0103083>.